Applied Clay Science xxx (2016) xxx–xxx

Contents lists available at ScienceDirect

Applied Clay Science

journal homepage: www.elsevier.com/locate/clay

Research paper

Adsorption of copper (II) onto cameroonian clay modified by non-thermal plasma: Characterization, chemical equilibrium and thermodynamic studies part A

Moïse Fouodjouo [a,b,*], Hervé Fotouo-Nkaffo [a], Samuel Laminsi [a], Felipe Antonio Cassini [b], Luís Octávio de Brito-Benetoli [b], Nito Angelo Debacher [b]

[a] Mineral Chemistry Laboratory, Department of Inorganic Chemistry, University of Yaoundé 1, P.O. Box 812, Yaoundé, Cameroon
[b] Chemistry Department, Federal University of Santa Catarina (UFSC), CEP 88040-900, Trindade, Florianopolis, SC, Brazil

ARTICLE INFO

Article history:
Received 22 October 2015
Accepted 25 September 2016
Available online xxxx

Keywords:
Clay
Non-thermal plasma
Adsorption equilibrium
Copper II ion

ABSTRACT

A cameroonian clay from Konhontsa'a (West Cameroon) has been treated in aqueous suspension by Non-thermal plasma (NTP) in order to modify its surface properties for a possible enhancement of effectiveness of heavy metals control in water by clays. FTIR spectroscopy, SEM-FEG analyses, X-ray diffraction and N_2 physisorption analyses were used to evaluate the physico-chemical, textural and crystalline properties changes in clay before and after plasma exposure. Copper (II) ions were used as heavy metal model for adsorption studies. XRD, elementary and FTIR analyses indicated that the clay is a disordered Kaolinite. XRD analysis also showed that, plasma treatment improved the crystallinity of the clay as a result of elimination of impurities by plasma actives species. However, the sheet structure remains unchanged. Furthermore, FTIR analysis reports that, none new functional group except oxygen was bonded to the clay after plasma exposure. SEM-FEG and N_2 physisorption analyses show that, the specific surface area and the volume of micropores decreased respectively from 98.40 to 35.43 $m^2 \cdot g^{-1}$ and from 0.23 to 0.079 $cm^3 \cdot g^{-1}$ by exposition to NTP. The adsorption capacity of Cu^{2+} by the clay decreased with plasma treatment but not significantly. The adsorption equilibrium was analyzed by Langmuir, Freundlich and Temkin models. Langmuir and Temkin models fit well the Cu^{2+} adsorption onto both samples. Adsorption of Cu^{2+} onto untreated and plasma treated clays was an exothermic process.

1. Introduction

Economic imperatives of productivity and profitability subjected to mining companies and mineral processing industries into products of higher added value significantly reflect the level of pollution by heavy metals. Removal of heavy metal ions from industrial effluents, drinking water and municipal wastewaters is a matter of serious concern due to their toxicity to various forms of life.

Among the variety of heavy metals pollutants of water, copper ions (II) appear and, as other heavy metals, they are not degradable and accumulate in the living beings. Although Cu^{2+} is essential trace nutrient that are required in small amount for catalysis of enzymatic activities of some microorganisms (Briand et al., 1997), they are highly toxic for aquatic and terrestrial organisms even in small dose (Camp, 1964). Copper reaches human body through drinking water and food chain causing various health troubles such as liver damage, Wilson disease and insomnia (Zhu et al., 2008). The limit concentration allowed is 3 $mg \cdot L^{-1}$ for surface water and 0.05 $mg \cdot L^{-1}$ for drinking water (Sandy et al., 2012). It becomes therefore necessary to refine wastewaters containing Cu^{2+} before their release in the environment. Several methods such electrochemical, chemical, ion-exchange, reverse osmosis, etc. sometime expensive and non-recyclable have been used with relative efficacies (Bilal et al., 2013). Adsorption using costless and efficient adsorbents such as activated carbons, biomass waste, clays etc. has shown its proofs (Bhattacharyya and Gupta, 2006; Lukman et al., 2013) and gave the possibilities for the regeneration of adsorbent and recovering of adsorbate using an appropriate technique.

Clays are hydrous alluminosilicates with small particle size (<2 μm), abundant in the nature and can have crystalline, amorphous, fibrous or platy structure. Their attractiveness for heavy metal adsorption resides in the high porous structure, high specific area, varied chemical structures, high chemical stability, high capacity of cation-exchange and, presence of Lewis and Bronsted acids in their surface (Bhattacharyya and Gupta, 2006; Eren, 2008).

The new challenge concerning clay application for environmental protection is to improve the absorbability. Many studies reported modifications of clays for a possible enhancement of pollutant binding capacities (Bhattacharyya and Gupta, 2006; Eren, 2008; Celis et al., 2000; Vieira et al., 2010; Abollino et al., 2003; Tiya-Djowe et al., 2013).

* Corresponding author at: Mineral Chemistry Laboratory, Department of Inorganic Chemistry, University of Yaoundé 1, P.O. Box 812, Yaoundé, Cameroon.

http://dx.doi.org/10.1016/j.clay.2016.09.028
0169-1317/

Most of them use chemicals and are expensive in terms of energy and built up. A promising, costless and environmentally friendly technology, called non-thermal plasma (NTP) can be a good alternative to improve heavy metal uptakes by clays.

Among NTP techniques, gliding arc plasma (glidarc) using humid air as flow gas specially attract our attention. The glidarc plasma in humid air atmosphere is rich of excited and radical species (•OH, •NO) which are highly reactive (Benstaali et al., 2002; Delair et al., 2001; Czernichowski, 1994) and can induce acid/base or oxidizing reactions with the aqueous suspension. Furthermore, secondary species such as HNO_3, peroxonitrous acid, H_2O_2 and O_3 also evidenced (Benstaali et al., 2002) in the aqueous solution can attack the suspension. A previous study reported that glidarc plasma induced surface modification of smectite clay (Tiya-Djowe et al., 2013) and the modification was attributed to acid and oxidizing properties of the Glidarc electric discharge species.

In this study we focused on the modification of cameroonian clay by glidarc plasma in humid air, and then, the adsorption process was investigated as a function of initial concentration of Cu^{2+} and plasma exposure time.

2. Experimental section

2.1. Materials

2.1.1. Reagents

Copper sulphate ($CuSO_4.5H_2O$) was purchased from Riedel-de-Häen(Germany) with purity 98%. The stock solution (5000 $mg \cdot L^{-1}$) of Cu^{2+} ions was prepared by dissolving 20.1 g of $CuSO_4 \cdot 5H_2O$ of molecular weight 249.68 $g \cdot mol^{-1}$ in 1000 mL of distilled water. The experimental solutions of desired concentration were prepared by diluting the stock solution with distilled water. The residual concentration of Cu^{2+} was determined by atomic absorption spectroscopy. Decimolar solution of HCl was used to adjust the pH in order to keep the solution acid and avoid precipitation.

2.1.2. Clay

The clay material used in the present study, was collected from Konhontsa'a, a small town in Bamboutos Division located in the West Cameroon Region (5°41″N and 10°13″E). The sample was washed with deionized water and the clay fraction (<2 μm) was separated by siphonation, decantation and dry in the oven at 105 °C for 24 h. Then, was kept in hermetically closed glass bottle for further uses.

2.2. Methods

2.2.1. Plasma treatment of clay

The glidarc device used for clay treatment was described previously. It is derived from the original device described by Czernichowski (1994). Fig. 1 presents a scheme of the experimental device. When a suitable voltage (5–10 kV) and electric current (160 mA) (Hnatiuc, 2002) are applied between two aluminum divergent electrodes, an electric arc forms at the shortest electrode gap (3 mm) and glides along the electrode's axis pushed on by a gas flow (humid air). The arc length increases on moving and its temperature decreases, so that the arc turns from thermal plasma to quenched plasma on breaking into a plume. A new arc then forms at the narrowest gap and the cycle resumes as a large plasma plume. The plasma plume leaks the clay suspension brought to its contact at overall room temperature and pressure close to atmospheric conditions (Czernichowski, 1994). The electric energy is transferred to gas (air) molecules which become excited and are broken into radicals giving highly reactive species such as HO• and NO• (Benstaali et al., 2002; Delair et al., 2001). The plasma plume is close enough to the liquid target, so that it leaks the liquid surface, and allow the chemical reaction to take place at the plasma-solution interface (Eqs. (1) to (6)) (Delair et al., 2001).

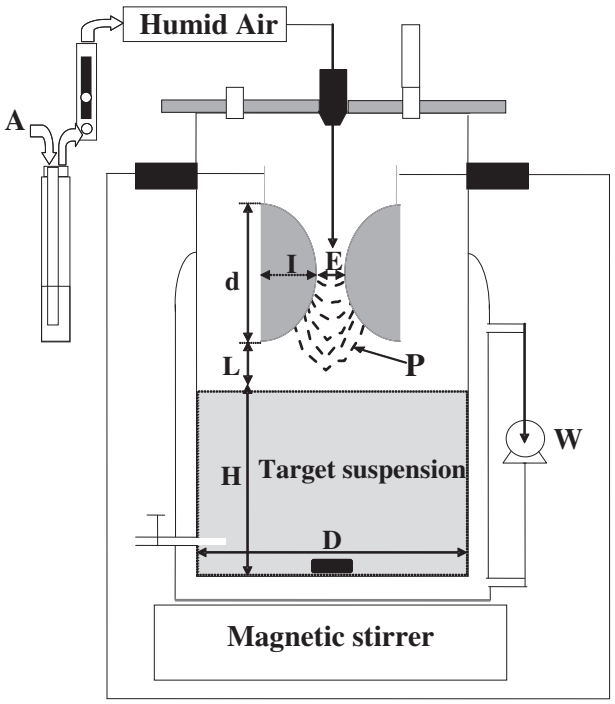

Fig. 1. Experimental setup of glidarc plasma. (A = air entrance; E = inter-electrode gap of 3 mm; I = electrode ray of 2 cm; d = electrode length of 7 cm; L = distance between electrodes and target surface of 1.5 cm; D = reactor diameter of 8 cm; H = height of solution in the reactor 10 cm; W = water pump).

$$H_2O + e^- \rightarrow H\bullet + OH\bullet + e^- \quad (1)$$

$$O_2 + e^- \rightarrow O(3P) + O(1D) + e^- \quad (2)$$

$$N_2 + e^- \rightarrow N(4S) + N(2D) + e^- \quad (3)$$

$$N(2D) + O_2 \rightarrow NO\bullet + O \quad (4)$$

$$H\bullet + O_2 \rightarrow HO_2^{\bullet} \quad (5)$$

$$HO_2^{\bullet} + NO\bullet \rightarrow NO_2 + OH\bullet \quad (6)$$

10 g of clay was introduced into the reactor containing 430 mL of distilled water. The flow rate of feeding gas (humid air) was set at the optimized value of 800 $L \cdot h^{-1}$ with a flow-meter connected to the air compressor. The electric discharge was then initiated by a switch connected to the high voltage generator. The working power was set at 1600 W.

A magnetic stirrer was employed in order to provide agitation, preventing the accumulation of solids at the bottom, improving the convection due to airflow and ultimately, avoiding diffusion control. Treatment was carried out in a closed batch reactor for different times (0–150 min). The reactor is equipped with a cooling system to avoid evaporation and the temperature was kept constant at 26 ± 0.1 °C for all treatments.

Each aliquot was named KON-t, where *t* (in minutes) represents the exposure time to the plasma discharge. The sample Kon-00 refers to the pristine clay (clay non-exposed to plasma discharge). After each time interval chosen (i.e. *t*), the discharge was switched off and the suspension clay was recovered and washed with deionized water and then, separated using vacuum filtration. The solid sample obtained was then dried in an oven at 105 °C for 24 h. Out of the oven, samples (KON-00

Please cite this article as: Fouodjouo, M., et al., Adsorption of copper (II) onto cameroonian clay modified by non-thermal plasma: Characterization, chemical equilibrium and thermodynamic studies part A, Appl. Clay Sci. (2016), http://dx.doi.org/10.1016/j.clay.2016.09.028

and KON-30) were crushed, sieved and kept into hermetically closed bottles for further use.

2.2.2. Batch adsorption experiments

The adsorption experiments were carried out in 250 mL Erlenmeyer flasks by mixing together a constant amount of clay with a constant volume of aqueous solution of Cu^{2+}. The contents in the flasks were agitated by placing them in a constant temperature water bath thermostat for a known time interval. The mixture was then centrifuged (4000 rpm) and residual Cu^{2+} in the supernatant liquid was determined by atomic absorption spectroscopy, as mentioned above. In the first series of experiments, the samples were triplicated and it was observed that there was <5% variability in the results. It was then useless to triplicate the experiments throughout the study. The uptake per mg of adsorbent, q and the percentage of Cu^{2+} adsorbed, *%Ads*, were calculated using Eqs. (7) and (8), as follows:

$$q = \frac{(C_0 - C_f)}{m} V \tag{7}$$

$$\%Ads = \frac{(C_0 - C_f)}{C_0} 100 \tag{8}$$

where q is the adsorption capacity ($mg \cdot g^{-1}$), C_0 and C_f are the initial and final copper (II) concentrations, respectively (expressed in $mg \cdot L^{-1}$), m is the adsorbent dosage (g) and V is the solution volume (mL).

2.2.3. Adsorbent characterization

XRD measurements were done with Enraf-Nomnius Analytical X-ray spectrometer (CADE-4) using CuKα radiations (λ = 1.5418 Å). Fourier transform infrared (FTIR) spectra were recorded in the wave number range of 4000–400 cm^{-1} using a Perkin Elmer FT-IR (KBr pellets method) to determine the presence of functional groups inserted on the clay before and after plasma treatment. The specific surface area and porosity of the samples were determined by nitrogen adsorption/desorption isotherms measured at 77 K in a Micromeritics ASAP 2020 apparatus. Before analysis, the samples were degassed at 350 °C for 2 h. The surface area was calculated by the BET method using N_2 adsorption isotherm data (Brunauer et al., 1938). The micropore volume was obtained from the amount of N_2 adsorbed at a pressure of 0.1 atm, and the mesopore volume was calculated by subtracting the amount adsorbed at 0.1 atm from that at 0.95 atm. The total pore volume was determined by the liquid volume at a relative pressure of 0.99 atm (Dubinin and Radushkevich, 1947).

The micro-morphologies and chemical composition of materials were obtained using high-resolution scanning electron microscopy (SEM-FEG).

3. Results and discussions

3.1. Characterization

3.1.1. XRD analysis

Diffractograms of KON-00 and KON-30 are shown in Fig. 2. It can be seen that all the major kaolinite reflections appeared in both diffractograms (Liew et al., 1985). However the diffractograms showed other different peaks due to the presence of different minerals other than kaolinite minerals. The peak appearing at 10.01 Å (Fig. 2) is assigned to the (002) reflection of a mica type mineral. The (020) reflection of kaolinite at 4.46 Å should be lower than the (1 $\bar{1}$ 0) peak at 4.35A. The relative height of this peak is a likely result of the overlapping with the (110 and 111) reflections of the mica-type mineral. The peak at 4.26 Å and 3.34 Å are assigned to the (110) and (101) reflections of quartz which means that KON-00 and KON-30 contain silica. The appearance of the (060) reflection at d = 1.49 Å indicates that the sample is a dioctahedral mineral (Gupta and Bhattacharyya, 2006). The peaks of reflexions ranged between the 2θ angles of 19° and 22° showed poor resolutions as consequence of the lower crystallinity index of the original material. The peak ranges at 2θ = 26.9° confirm the presence of morganite in the material. All this, together with the broadening of the peaks of the other non-basal reflections suggests that the solid sample is a disordered kaolinite clay in nature (Gupta and Bhattacharyya, 2006). This particularity is an advantage for adsorption capacity of samples.

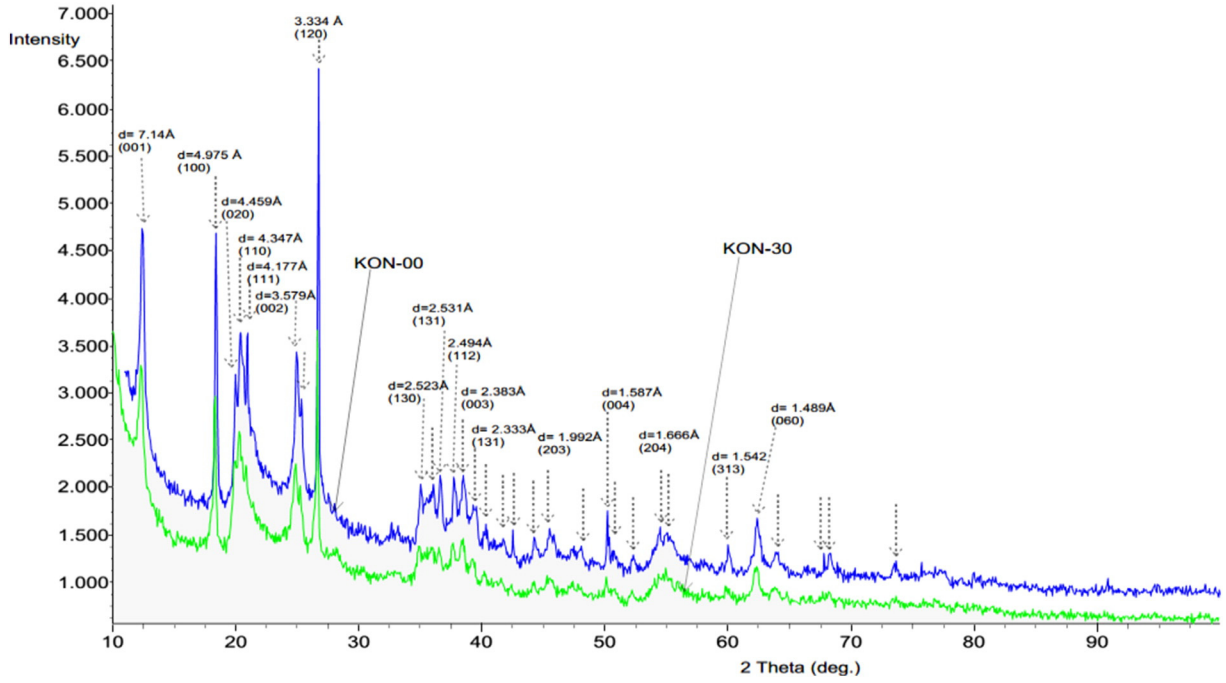

Fig. 2. XRD patterns of KON-00 (blue line) and KON-30 (green line). (For interpretation of the references to color in this figure legend, the reader is referred to the web version of this article.)

Please cite this article as: Fouodjouo, M., et al., Adsorption of copper (II) onto cameroonian clay modified by non-thermal plasma: Characterization, chemical equilibrium and thermodynamic studies part A, Appl. Clay Sci. (2016), http://dx.doi.org/10.1016/j.clay.2016.09.028

Table 1
Elemental composition of KON-00 and KON-30.

Atom %							
Elements	C Kα	O Kα	Al K_α	Si K_α	Ti K_α	Fe K_α	Fe L_α
KON-00	24.22	40.09	18.09	15.67	1.74	–	0.18
KON-30	–	70.48	15.97	11.44	0.83	1.28	–

The comparison between KON-00 and KON-30 showed that, glidarc plasma treatment in aqueous suspension introduced some changes into the crystal structure of the clay material. In fact d_{001}, d_{100}, $d_{1\bar{1}0}$, $d_{11\bar{1}}$, d_{002}, d_{120} and d_{004} respectively at 7.14, 4.97, 4.34, 4.17, 3.57, 3.34 and 1.58 Å increased in intensity after plasma exposure. This may be related to the increase of crystallite size (Veli and Alyüz, 2007) and/or the degradation by plasma chemical species (OH• or H_2O_2) of traces of organic impurities generally amorphous (Delair et al., 2001; Czernichowski, 1994). Furthermore some new reflections appeared at $2\theta = 42.5°$ and 68.2°. This can be attributed to the oxidation of some iron, as and a consequence shifts the original spectral wave length. Table 1 presents the elemental composition KON-00 and K0 N-30. It can be seen that Fe L_α was utterly converted to Fe K_α corresponding to the improvement of the crystallinity of the plane (110) and (100).

3.1.2. Morphology

The SEM-FEG micrographs of untreated (KON-00) and plasma treated (KON-30) clay samples are presented in Fig. 3 with different magnetisations. It can be seen that, the clay particles sizes increased after exposure to plasma (see Fig. 3a and d). Fig. 3b showed an amorphous surface and, an irregular flaky morphology with random orientation. Fig. 3d has shown well-bond particle, several flaky particles stacked together, but was less amorphous compared to Fig. 3b.

3.1.3. FTIR spectroscopy

Fig. 4 presents all the FTIR absorption bands of both materials studied. In the O—H stretching region, KON-00 and KON-30 showed three significant bands at 3696 cm^{-1}, 3621 cm^{-1} and 3527 cm^{-1} corresponding to Al—OH and Si—OH stretching. The band at 3696 cm^{-1} is related to Al—OH symmetric stretching whereas the band at 3621 cm^{-1} is attributed to inner hydroxyl groups, located between the tetrahedral and octahedral sheets. Out-of-plane stretching vibrations appeared at 3527 cm^{-1}. High amount of water physisorbed on the surface of the clay is assigned to the band which appeared at 3445 cm^{-1} (Hameed and Ahmad, 2009; Almeida et al., 2009). The band at 1631.06 cm^{-1} can be attributed to the bending vibration mode of physisorbed water on the surface of free silica produced due to leaching (Almeida et al., 2009). The peaks at 1100.77 cm^{-1} and 1032 cm^{-1} are due to Si—O stretching vibrations. The bands at 913.35 cm^{-1}, 795.77 cm^{-1}, 694 cm^{-1} and 538 cm^{-1} can be assigned to the Al—Al—OH and Si—O—Al vibrations of the clay sheet. However perceptible changes were observed in NTP-treated clay. Plasma treatment increased the intensities —OH stretching bands at the region of 3445 cm^{-1}, 1032 cm^{-1}, 913.35 cm^{-1}, 797 cm^{-1}, 694 cm^{-1}, 538 cm^{-1} and 469 cm^{-1}. The peaks at wavenumber interval of 1631.06–900 cm^{-1} were shifted from its initial position after the NTP treatment. KON-30 showed a new peak at wavenumber 1403.57 cm^{-1}. This may be due to the fixation of oxygen containing groups by NTP due to OH•, H_2O_2, $O2^{\bullet -}$, etc. produced by the discharge (Yavuz and Saka, 2013; Delair et al., 2001; Czernichowski, 1994).

3.1.4. Specific surface area and pore structure

The effects of plasma treatment on the N_2 adsorption desorption and pore size distribution is presented in Fig. 5. The concavity of the adsorption isotherms of both materials almost persists throughout their course (Fig. 5a). These isotherms were classified as type IV on the basis of IUPAC recommendations and are typical of mesoporous structures (Gregg and Sing, 1982). The hysteresis loops of untreated and plasma treated clay (Fig. 5a) were similar to type *H*3, typical of agglomerates of plate-like particles containing slit-shaped pores and a capillary decondensation of N_2 in clays in-between-sheets lamellar mesopores (Tiya-Djowe et al., 2013; Panda et al., 2010). The isotherms also suggested the presence of some micro and macroporosity. The adsorption/desorption isotherm sharp remained unchanged after the plasma treatment; this indicates that the interlayer space of clay particles was not affected. From Table 2, it can be observed that, plasma treatment

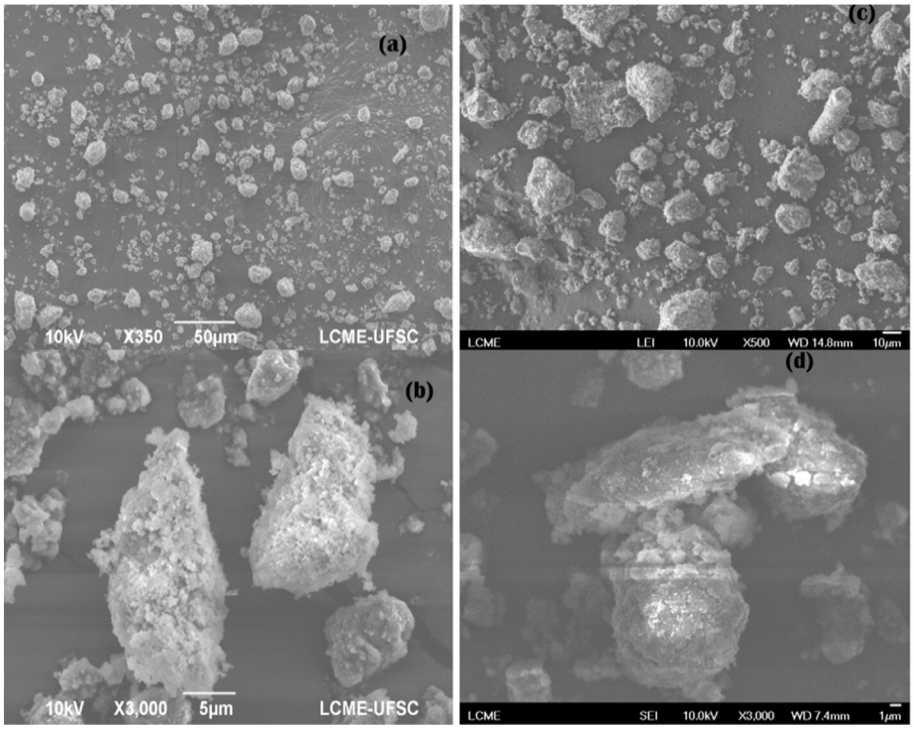

Fig. 3. SEM-FEG images; (a) and (b) KON-00, (c) and (d) KON-30.

Please cite this article as: Fouodjouo, M., et al., Adsorption of copper (II) onto cameroonian clay modified by non-thermal plasma: Characterization, chemical equilibrium and thermodynamic studies part A, Appl. Clay Sci. (2016), http://dx.doi.org/10.1016/j.clay.2016.09.028

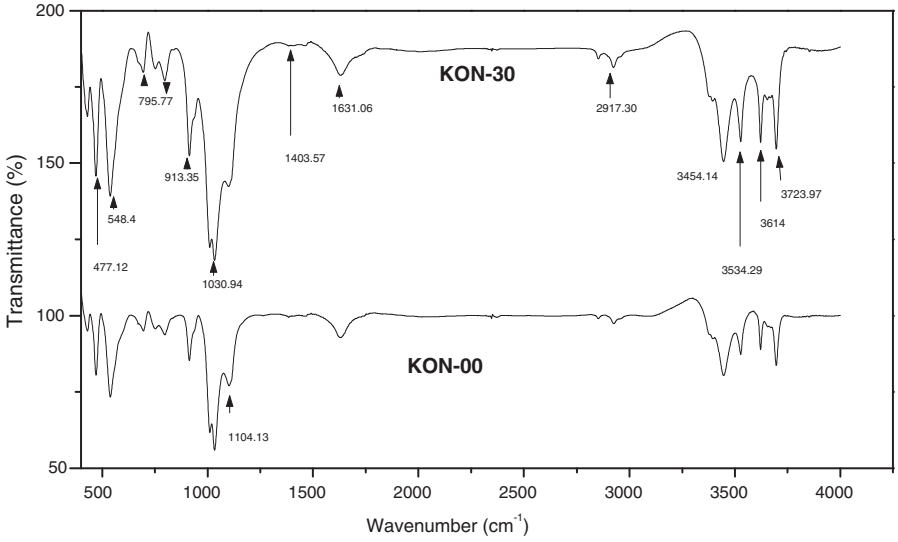

Fig. 4. Infrared spectra of KON-00 and KON-30.

decreased the specific surface area (from 98.40 to 35.43 $m^2 \cdot g^{-1}$) and the pore volume (from 0.23 to 0.079 $cm^3 \cdot g^{-1}$) of the clay. However, the average radius of pore remained unchanged. The pore size distributions of untreated and plasma treated samples showed sharp peaks at a radius 21.36 Å and 21.57 Å, respectively (Fig. 5b), and thus consisting of mesoporous (Gregg and Sing, 1982). In KON-00 the maximum average pore radius found was 292 Å whilst in the plasma treated sample, it was 423 Å, this shows that the plasma treatment increased the number of existing macropores and consequently the decrease of existing micropore number. The direct consequence of this increase of the number of macropores was the reduction of the interaction between the molecules of N_2 gas with the atoms or ions constituting the clay and thus the reduction of specific surface area. The mesopores, more numerous were not affected.

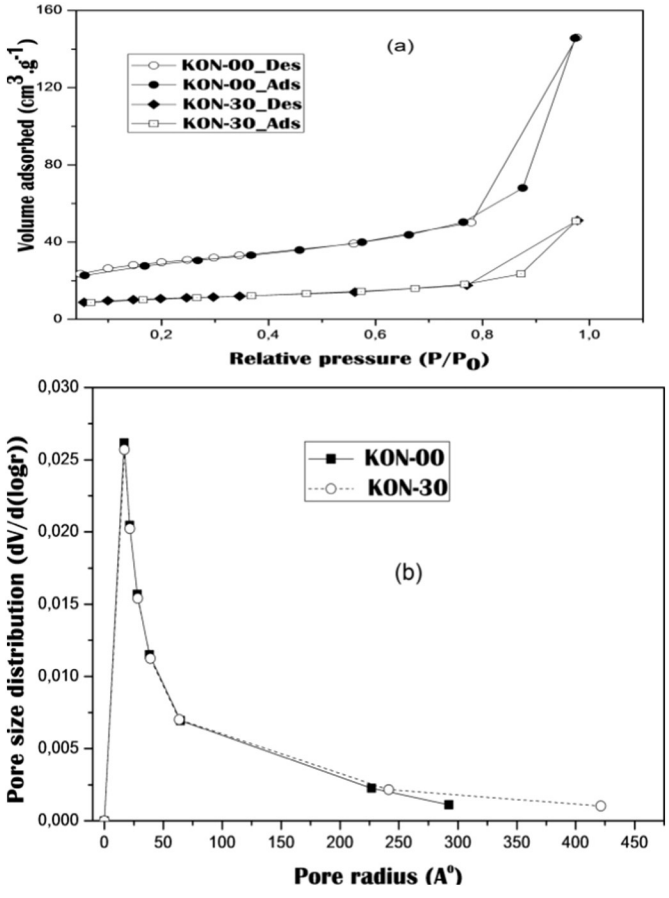

Fig. 5. Pore structure of KON-00 and KON-30: (a) N_2 adsorption/desorption isotherm, (b) pore size distribution.

3.2. Adsorption studies

3.2.1. Effect of adsorbent dosage

In order to determine the adsorbent dosage for optimal adsorption of Cu^{2+} ions onto KON-00 and KON-30, 50 mL of Cu^{2+} ions was put in contact with a given mass of adsorbent which has been varied from 0.1 g to 0.5 g. The time of contact was three min and the solution was mixed at 200 rpm. From Fig. 6 it can be seen that, the amount of Cu^{2+} adsorbed per unit mass (qe) of those adsorbents at equilibrium decreased with an increase in the adsorbent dosage. This can be due to the competitive adsorption between the free adsorption sites and the saturated adsorption sites. Moreover, although the number of adsorption sites per unit mass of adsorbent should remain constant independently of the total adsorbent mass, increasing the adsorbent amount in a fixed volume reduces the number of available sites as the effective surface area is likely to decrease (Gupta and Bhattacharyya, 2006)

3.2.2. Effect of contact time

Fig. 7 depicts the evolution of the amount of Cu^{2+} uptake with the contact time. It came out that, the adsorption capacity of Cu^{2+} increased with time and reached equilibrium after 3 min. The adsorption is quiet fast and attained a maximum after 1 min of contact, then followed a gradual decrease with time until it reached equilibrium. This may be due to the fact that, at the beginning, the surface adsorption sites were readily available and consequently, adsorption proceeded at very high rate, then, with increasing coverage, the number of sites became less and Cu^{2+} ions had to fiercely compete among themselves for getting

Table 2
Surface area, pore volume and average pore radius of KON-00 and KON-30.

Material	KON-00	KON-30
Specific surface area ($m^2 \cdot g^{-1}$)	98.40	35.43
Pore volume ($cm^3 \cdot g^{-1}$)	0.23	0.079
Average pore radius (Å)	45.90	44.72

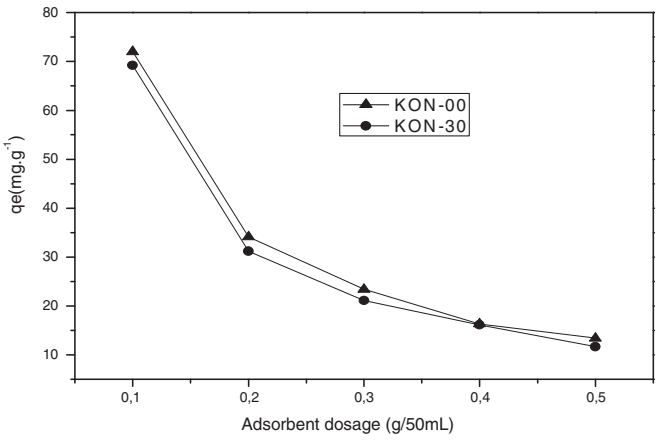

Fig. 6. Effect of adsorbent dosage ($C_0 = 500\ mg{\cdot}L^{-1}$, pH = 5.7 ± 0.1, T = (29 ± 0.1)*K*).

adsorbed (Weber and Chakkravorti, 1974). Furthermore, the migration of Cu^{2+} ions from the adsorbent to the solution between 1 and 3 min can be attributed to the phase of establishment of a dynamic chemical equilibrium. This two-stage metal ion uptake can also be explained as adsorption occurring onto two different types of binding sites on the adsorbent particles (Arias and Sen, 2009).

3.2.3. Effect of initial concentration

Fig. 8 shows the adsorption uptake versus initial concentration for an equilibrium time of 3 min. The amount of metal removed at equilibrium increased from 71 $mg{\cdot}g^{-1}$ to 195 $mg{\cdot}g^{-1}$ for KON-00 and from 56.6 $mg{\cdot}g^{-1}$ to 183.2 for KON-30 with the increase in metal concentration from 500 $mg{\cdot}L^{-1}$ to 3000 $mg{\cdot}L^{-1}$. It is clear that the removal of heavy metal depends on the initial concentration. This is due to the fact that, the initial Cu(II) concentration provided the necessary driving force to overcome the resistances to the mass transfer of Cu^{2+} ions between the solution and adsorbent (Hameed and Ahmad, 2009).

3.2.4. Influence of plasma exposure time of raw clay

The effect of plasma exposure time on the amount of Cu^{2+} ions uptake ($mg{\cdot}g^{-1}$) is presented by Fig. 9. It can be seen that plasma treatment reduced the adsorption capacity of the clay. The decrease was gradually important with the time from 0 to 30 min where it did not vary anymore with increase of exposure time. This result confirmed

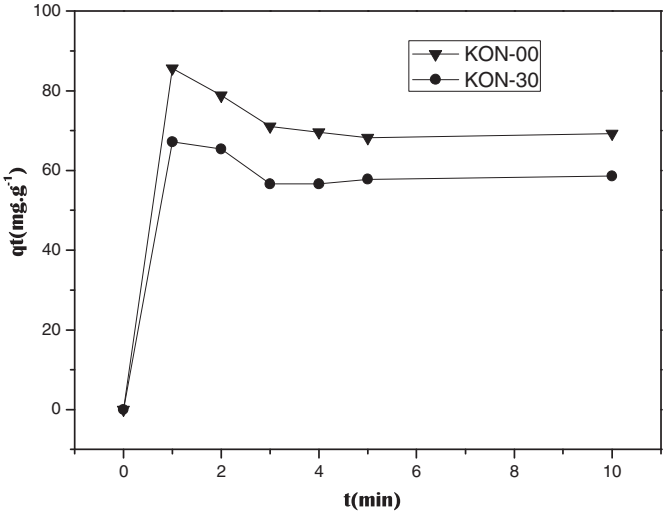

Fig. 7. Effect of contact time ($C_0 = 500\ mg{\cdot}L^{-1}$, $m_{adsorbent} = 0.1$ g, pH = 5.7 ± 0.1, $V = 50$ mL, T = (298 ± 0.1)*K*).

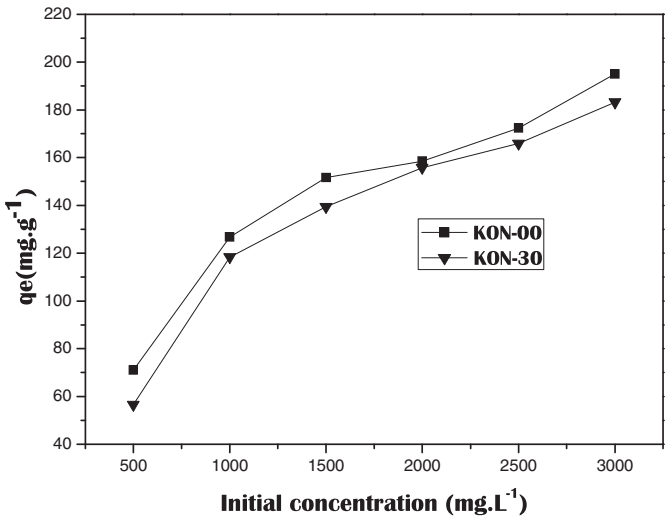

Fig. 8. Influence of initial concentration ($m_{adsorbent} = 0.1$ g, pH = 5.7 ± 0.1, $V = 50$ mL, T = (298 ± 0.1)*K*, adsorption time = 3 min).

the changes in characteristics observed in the paragraph above. This is due to the reduction of specific surface area and amorphous character with exposure to plasma.

3.2.5. Adsorption equilibrium

The adsorption isotherm study points out how the adsorbate distributes between the solution and the adsorbent when the adsorption process is at equilibrium state. The analysis of the isotherm data by fitting them with different isotherm models is an unavoidable step to find the appropriate model that can be used for design the process (Almeida et al., 2009). In this work, Langmuir, Freundlich and Temkin isotherms were used to fit the experimental data.

The Langmuir isotherm is represented by the linear equation (Eq. (9)) (Langmuir, 1918) and the dimensionless constant called equilibrium parameter R_L (Eq. (10)) (Weber and Chakkravorti, 1974):

$$\frac{Ce}{q_e} = \frac{Ce}{q_m} + \frac{1}{bq_m} \tag{9}$$

$$R_L = \frac{1}{1 + bC_0} \tag{10}$$

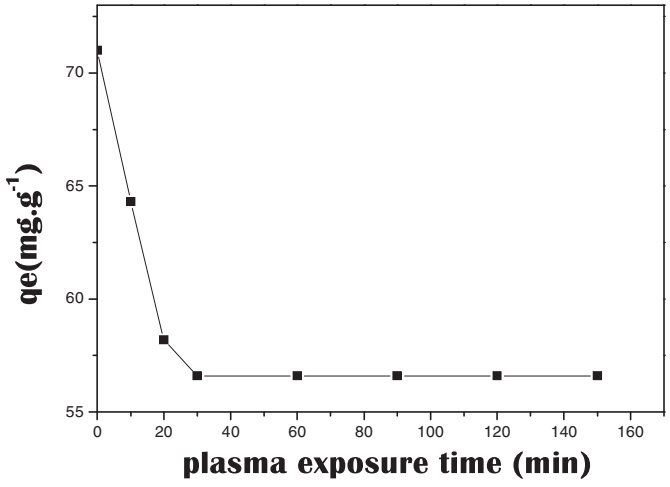

Fig. 9. Influence of plasma treatment time. ($C_0 = 500\ mg{\cdot}L^{-1}$, $m_{adsorbent} = 0.1$ g, pH = 5.7 ± 0.1, $V = 50$ mL, T = (298 ± 0.1)*K*, adsorption time = 3 min).

Please cite this article as: Fouodjouo, M., et al., Adsorption of copper (II) onto cameroonian clay modified by non-thermal plasma: Characterization, chemical equilibrium and thermodynamic studies part A, Appl. Clay Sci. (2016), http://dx.doi.org/10.1016/j.clay.2016.09.028

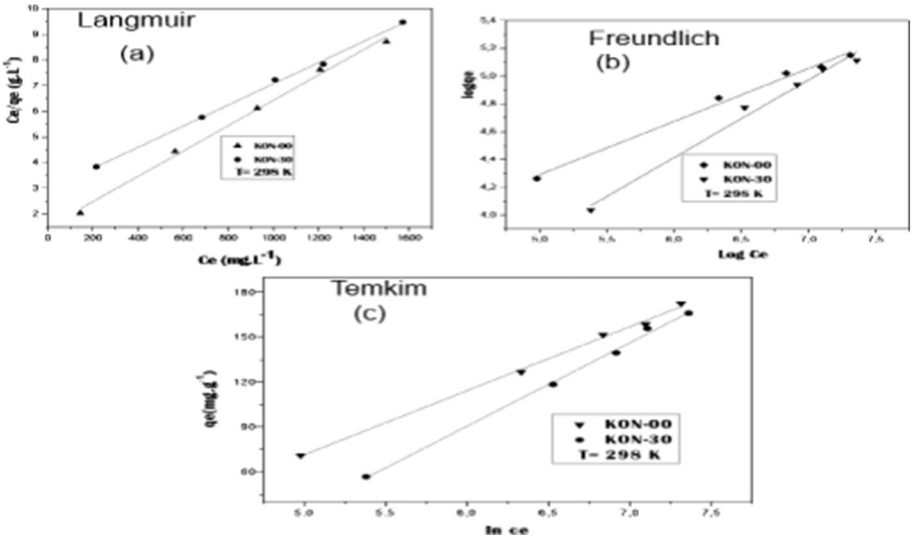

Fig. 10. Adsorption isotherm of Cu^{2+} adsorption onto KON-00 and KON-30 ($m_{adsorbent}$ = 0.1 g, T = (298 ± 0.1) K, pH = 5.7 ± 0 0.1); (a) Langmuir isotherm, (b) Freundlich isotherm, (c) Temkim isotherm.

Where C_e and C_0 ($mg \cdot L^{-1}$) are the equilibrium and highest Cu^{2+} concentration, q_e ($mg \cdot g^{-1}$) the amount of adsorbate retained per unit mass of adsorbent, and q_m and b are the Langmuir constants related to adsorption capacity and rate of adsorption, respectively. When Ce/qe was plotted against Ce, a straight line with slope $1/q_m$ was obtained (Fig. 10a), indicating that the adsorption of Cu^{2+} on KON-00 and KON-30 follows the Langmuir isotherm. In fact, the value of RL indicates the type of the isotherm to be either unfavorable (RL > 1), linear (RL = 1), favorable (0 < R_L < 1) or irreversible (RL = 0). The values of R_L and Langmuir constants (b and q_m) were calculated from this isotherm and their values are listed in Table 3.

The linear form of Freundlich equation (Freundlich, 1906) is:

$$\ln q_e = \ln K_F + \frac{1}{n} \ln C_e \quad (11)$$

where K_F ($mg \cdot g^{-1} \cdot L^{1/n} \cdot mg^{-1/n}$) and n are Freundlich constants. The parameters n and K_F inform about the favourability of adsorption process and the adsorption capacity of the adsorbent. The plot of ln qe versus ln C_e (Fig. 10b) gave straight lines with slope 1/n. From Fig. 10b, it can be said that the adsorption of Cu^{2+} also followed the Freundlich isotherm. KF and n were determined and listed in Table 3.

The equation below represents the linear form of Temkin isotherm (Tempkin and Pyzhev, 1940):

$$q_e = B \ln A + B \ln C_e \quad (12)$$

Table 3
Isotherm parameters for Cu (II) ions by KON-00 and KON-30.

Isotherm	Parameters	T = 298 K	
		KON-00	KON-30
Langmuir	q_m ($mg \cdot g^{-1}$)	242.72	202.43
	b ($L \cdot mg^{-1}$)	$1.40 * 10^{-4}$	$3.31 * 10^{-4}$
	R^2	0.9972	0.9940
	R_L	0.21	0.54
Freundlich	K_F ($mg \cdot g^{-1} \cdot L^{1/n} \cdot mg^{-1/n}$)	6.89	2.90
	n	2.63	1.79
	R^2	0.9886	0.9832
Temkin			
	B	42.79	55.80
	A ($L \cdot g^{-1}$)	$3.57 * 10^{-2}$	$1.31 * 10^{-2}$
	R^2	0.9964	0.9965

Where $B = \frac{RT}{b}$, is a constant relative to heat adsorption and A ($L \cdot g^{-1}$), the equilibrium binding constant corresponding to the maximum binding energy. The plot of qe versus ln C_e gave straight lines and that shows that, the adsorption of Cu^{2+} ions also followed Temkim isotherm. A and B were calculated and listed in Table 3.

The values of R_L for KON-00 and KON-30 listed in Table 3 are in the interval 0 < R_L < 1. The values of R^2 for Langmuir and Temkin isotherm models were >0.99 and the maximum binding energy for both materials at 298 K were relatively low. Langmuir and Temkin Isotherms models are the best which fitted well the adsorption equilibrium of Cu^{2+} ions onto raw and treated clays. Similar results were obtained by Yavuz et al., Bhattacharyya et al. and Gupta et al. (Bhattacharyya and Gupta, 2006; Gupta and Bhattacharyya, 2006; Yavuz et al., 2003). Moreover, data listed in Table 3 showed that the plasma treatment influence the adsorption equilibrium.

3.2.6. Thermodynamic studies

The effect of temperature on adsorption capacity of KON-00 and KON-30 at equilibrium time was studied at five different temperatures for a fixed initial concentration of 500 ppm. Fig. 11a shows that the amount of Cu^{2+} ions adsorbed on both clay samples remained almost constant when the temperatures changed from 298 K to 303 K and then, decreased with increasing temperature of the solution from 308 K. This is mainly because of decreased surface activity suggesting that adsorption of Cu^{2+} onto the clay was an exothermic process. With increase of temperature, the attractive forces between the clay surface and metal ions are weakened and the adsorbate tendency to escape from the adsorbent to the solution increases. Similar results were reported by Bhattacharyya and Gupta (2006, 2008) and Arias and Sen (2009). The Gibb's free energy (ΔG^0), enthalpy (ΔH^0) and entropy (ΔS^0) changes for Cu^{2+} ions adsorption have been determined using Eq. (13) and also from slope and intercept of a plot of log (qe/Ce) versus 1/T according to Eq. (14) (Fig. 11b) (Panda et al., 2010; Bhattacharyya and Gupta, 2008). The three thermodynamic parameters are tabulated in Table 4.

$$\Delta G^0 = \Delta H^0 - T\Delta S^0 \quad (13)$$

$$\log\left(\frac{q_e}{C_e}\right) = \frac{\Delta S^0}{2.303\ R} + \frac{-\Delta H^0}{2.303\ RT} \quad (14)$$

Where q_e ($mg \cdot g^{-1}$) is the amount of metal ions adsorbed on the clay samples at equilibrium, Ce is the equilibrium concentration

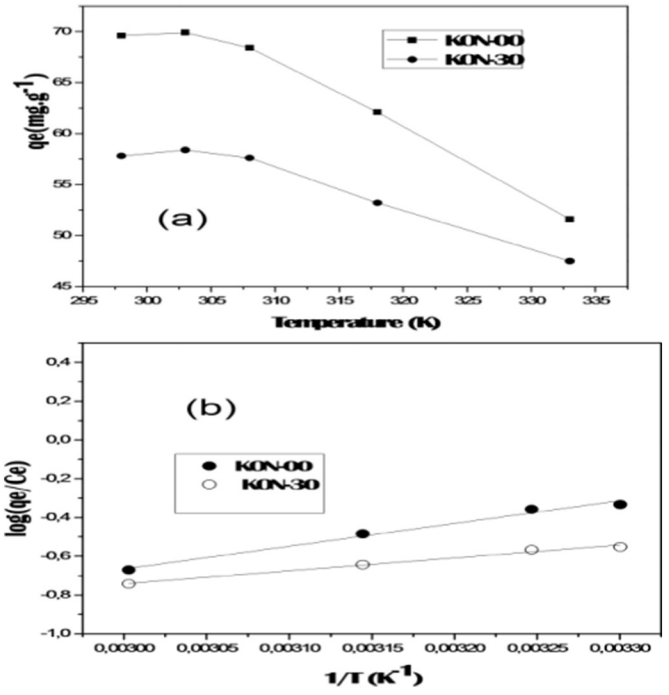

Fig. 11. Effect of temperature on sorption of Cu^{2+} ions.

$(mg \cdot L^{-1})$ and T is temperature in K and R is the gas constant $(8.314\ J \cdot mol^{-1} \cdot K^{-1})$. ΔG^0, ΔH^0 are expressed in $kJ \cdot mol^{-1}$ and ΔS^0 in $kJ \cdot mol^{-1} \cdot K^{-1}$

The negative values of ΔG^0 showed a spontaneous physical adsorption of Cu^{2+} on the clay, indicating that this system did not gain energy from external resource (Bhattacharyya and Gupta, 2008; Vimonses et al., 2009). The increase in ΔG^0 with increase in temperature indicated less efficient adsorption at higher temperature. The enthalpy change ΔH^0 and entropy change ΔS^0 for both samples were negative, suggesting the exothermic nature of the process and the decrease in randomness at the solid/liquid interface (Vimonses et al., 2009). The untreated clay and plasma treated one presented almost the same thermodynamic parameters with little improvement in KON-00.

4. Conclusion

Cameroonian clay from Konhontasa'a (West Cameroon) has been treated in aqueous suspension by NTP in order to modify its surface properties for a possible enhancement of heavy metals control in water by clays. XRD, elementary and FTIR analysis indicated that, the clay is a disordered Kaolinite. XRD and elementary analyses have also shown that, plasma treatment removed the impurities and improved the crystallinity of the original clay. It is also found that, the surface area decreased and none new functional group was brought by plasma treatment. The maximum pore radius found was 292 Å for untreated clay and 423 for 30 min plasma treated clay. However, the sheet structure remains unchanged. Adsorption of Cu^{2+} ions showed that plasma treatment decreases the adsorption capacity of the clay. The adsorption capacity of Cu^{2+} decreased of about 21% after 30 min of plasma exposure. The results of adsorption studies of Cu^{2+} also indicated that the adsorption capacity of the clay whether treated or not was strongly affected by the initial concentration, the adsorbent dosage and temperature. The adsorption capacity increased with increase in initial concentration but decreased with increase in adsorbent dosage or temperature. Langmuir and Temkin isotherms fitted well the experimental data for both samples. The maximum adsorption capacities calculated with Langmuir isotherm model were respectively 242.72 $mg \cdot g^{-1}$ and 202.43 $mg \cdot g^{-1}$ for untreated and 30 min plasma treated clays. Thermodynamic studies have shown that the adsorption of Cu^{2+} ions onto the untreated and plasma treated clays is an exothermic process. The adsorption of Cu^{2+} onto the clay was fast and the equilibrium was reached after 3 min.

Table 4
Thermodynamic parameters for the adsorption of Cu^{2+} ions at different temperatures.

Material	KON-00 (R^2 = 0.9842)			KON-30 (R^2 = 0.9801)		
Temperature (K)	ΔG^0	ΔH^0	ΔS^0	ΔG^0	ΔH^0	ΔS^0
303	−4.23	−28.47	−0.08	−4.17	−19.92	−0.052
308	−3.02	−36.98	−0.11	−2.78	−30.29	−0.089
318	−2.22	−56.29	−0.17	−2.36	−34.80	−0.102
333	−1.82	−78.41	−0.23	−1.61	−47.23	−0.137

Acknowledgments

The authors of this work are grateful to TWAS-CNPq (190088/2012-5) doctoral programme for the financial support, the LCME-UFSC for help with the analysis and the Laboratory of Interfacial Electrochemistry and Analytical Chemistry (LEICA) of the University of Rouen for the plasma equipments provided.

References

Abollino, O., Aceto, M., Malandrino, M., Sarzanini, C., Mentasti, E., 2003. Adsorption of heavy metals on Na-montmorillonite: effect of pH and organic substances. Water Res. 37, 1619–1627.
Almeida, C.A.P., Debacher, N.A., Downs, A.J., Cottet, L., Mello, C.A.D., 2009. Removal of methylene blue from colored effluents by adsorption on montmorillonite clay. J. Colloid Interface Sci. 332, 46–53.
Arias, F., Sen, T.K., 2009. Removal of zinc metal ion (Zn^{2+}) from its aqueous solution by kaolin clay mineral: a kinetic and equilibrium study. Colloids Surf. A Physicochem. Eng. Asp. 48, 100–108.
Benstaali, B., Boubert, P., Cheron, B.G., Addou, A., Brisset, J.L., 2002. Density and rotational temperature measurements of the OH• and NO• radicals produced by a gliding arc in humid air. Plasma Chem. Plasma Process. 22, 553–571.
Bhattacharyya, K.G., Gupta, S.S., 2006. Kaolinite, montmorillonite, and their modified derivatives as adsorbents for removal of Cu (II) from aqueous solution. Sep. Purif. Technol. 50, 388–397.
Bhattacharyya, K.G., Gupta, S.S., 2008. Adsorption of a few heavy metals on natural and modified kaolinite and montmorillonite: a review. Adv. Colloid Interf. Sci. 140, 114–131.
Bilal, M., Shah, J.A., Ashfaq, T., Gardazi, S.M.H., Tahir, A.A., Pervez, A., Haroon, H., Mahmood, Q., 2013. Waste biomass adsorbents for copper removal from industrial wastewater—a review. J. Hazard. Mater. 263 (2), 322–333.
Briand, L., Chobert, J.-M., Tauzin, J., Declerck, N., Léonil, J., Mollé, D., Tran, V., Haertle, T., 1997. Regulation of trypsin activity by Cu^{2+} chelation of the substrate binding site. Protein Eng. 10 (5), 551–560.
Brunauer, S., Emmett, P.H., Teller, E., 1938. Adsorption of gases in multimolecular layers. J. Am. Chem. Soc. 60, 309–319.
Camp, R.T., 1964. Water and Its Impurities. second ed. Reinhold, New York.
Celis, R., Hermosin, M.C., Cornejo, J., 2000. Heavy metal adsorption by functionalized clays. Environ. Sci. Technol. 34, 4593–4599.
Czernichowski, A., 1994. Gliding-arc application to engineering and environment control. Pure Appl. Chem. 66, 1301–1310.
Delair, L., Brisset, J.L., Cheron, B.G., 2001. Spectral, electrical and dynamical analysis of a 50 Hz air gliding arc. High Temp. Mater. Process. 5, 381–402.
Dubinin, M.M., Radushkevich, L.V., 1947. Equation of the characteristic curve of activated charcoal. Proc. Acad. Sci. USSR Phys. Chem. Sect. 55, 331–337.
Eren, E., 2008. Removal of copper ions by modified Unye clay, Turkey: J. Hazard. Mater. 159, 235–244.
Freundlich, H.M.F., 1906. Over the adsorption in solution. J. Phys. Chem. 57, 385–470.
Gregg, S.J., Sing, K.S.W., 1982. Adsorption, Surface Area and Porosity. second ed. Academic Press, London.
Gupta, S.S., Bhattacharyya, K.G., 2006. Adsorption of Ni(II) on clays. J. Colloid Interface Sci. 295, 21–32.
Hameed, B.H., Ahmad, A.A., 2009. Batch adsorption of methylene blue from aqueous solution by garlic peel, an agricultural waste biomass. J. Hazard. Mater. 164, 870–875.
Hnatiuc, E., 2002. Procédés électriques de mesure et de traitement des polluants. Lavoisier, Paris.
Langmuir, I., 1918. The adsorption of gases on plane surfaces of glass, mica and platinum. J. Am. Chem. Soc. 40, 1361–1403.
Liew, K.Y., Khoo, L.E., Bong, K.T., 1985. Characterization of bidor kaolinite and illite. Pertanika 8, 323–330.
Lukman, S., Essa, M.S., Mu'azu, M.D., Bukhari, A., Basheer, C., 2013. Adsorption and desorption of heavy metals onto clay natural material: influence of initial pH. J. Environ. Sci. Technol. 6, 1–15.

Please cite this article as: Fouodjouo, M., et al., Adsorption of copper (II) onto cameroonian clay modified by non-thermal plasma: Characterization, chemical equilibrium and thermodynamic studies part A, Appl. Clay Sci. (2016), http://dx.doi.org/10.1016/j.clay.2016.09.028

Panda, A.K., Mishra, B.G., Mishra, D.K., Singh, R.K., 2010. Effect of sulphuric acid treatment on the physico-chemical characteristics of kaolin clay. Colloids Surf. A Physicochem. Eng. Asp. 363, 98–104.
Sandy, M.V., Kurniawan, A., Ayucitra, A., Sunarso, J., Ismadji, S., 2012. Removal of copper ions from aqueous solution by adsorption using laboratories-modified bentonite (organo-bentonite). Front. Chem. Sci. Eng. 6, 58–66.
Tempkin, M.J., Pyzhev, V., 1940. Recent modifications to Langmuir isotherms. Acta Physiochim. USSR 12, 217–222.
Tiya-Djowe, A., Laminsi, S., Njopwouo, D., Acayanka, E., Gaigneaux, E.M., 2013. Surface modification of smectite clay induced by non-thermal gliding arc plasma at atmospheric pressure. Plasma Chem. Plasma Process. 33 (4), 707–723.
Veli, S., Alyüz, B., 2007. Adsorption of copper and zinc from aqueous solution by using natural clay. J. Hazard. Mater. 149, 226–233.
Vieira, M.G.A., Almeida, N.A.F., Gimenes, M.L., Da Silva, M.G.C., 2010. Removal of nickel on Bofe bentonite calcined clay in porous bed. J. Hazard. Mater. 176, 109–118.
Vimonses, V., Lei, S., Jin, B., Chow, C.W.K., Saint, C., 2009. Kinetic study and equilibrium isotherm analysis of Congo red adsorption by clay materials. Chem. Eng. J. 148, 354–364.
Weber, T.W., Chakkravorti, R.K., 1974. Pore and solid diffusion models for fixed-bed adsorbers. AICHE J. 20, 220–228.
Yavuz, Ö., Saka, C., 2013. Surface modification with cold plasma application on kaolin and its effects on the adsorption of methylene blue. Appl. Clay Sci. 85, 96–102.
Yavuz, O., Altunkaynak, Y., Guzel, F., 2003. Removal of copper, nickel, cobalt and manganese from aqueous solution by kaolinite. Water Res. 37, 948–952.
Zhu, B., Fan, T., Zhang, D., 2008. Adsorption of copper ions from aqueous solution by citric acid modified soybean straw. J. Hazard. Mater. 153, 300–308.

Please cite this article as: Fouodjouo, M., et al., Adsorption of copper (II) onto cameroonian clay modified by non-thermal plasma: Characterization, chemical equilibrium and thermodynamic studies part II, Appl. Clay Sci. (2016), http://dx.doi.org/10.1016/j.clay.2016.09.028